Desalination and Water Treatment
www.deswater.com

doi: 10.5004/dwt.2019.23593

150 (2019) 192–203
May

Synthesis and characterization of alumina-grafted acrylic acid monomer and polymer and its adsorption of phenol and p-chlorophenol

Maha T. Sultan[a], Hadi S. Al-Lami[b], Ammar H. Al-Dujiali[c,*]

[a]*Department of Chemistry, College of Education for Pure Science, Ibn Al-Haitham, University of Baghdad, Baghdad, Iraq, Tel. +964 770 984 9297; email: dr.maha.almahdawy@gamil.com*
[b]*Department of Chemistry, College of Science, University of Basrah, Basrah, Iraq, Tel. +964 770 737 7488; email: hadisalman54@yahoo.com*
[c]*Hamdi Mango Center for Scientific Research, The University of Jordan, Amman, P.O. Box 11942, Jordan, Tel. +962 796 629 774; email: ah.aldujaili@gmail.com*

Received 20 May 2018; Accepted 14 December 2018

ABSTRACT

Aluminum oxide (ALO) was grafted by acrylic acid monomer (AlO-AM) and then, it was polymerized to produce alumina grafted poly(acrylic acid) (AlO-AP). The prepared AlO-AM and AlO-AP were characterized by Fourier-transform infrared, differential scanning calorimetry , thermogravemetric analyzer and particle size distribution. Adsorption equilibrium isotherms, adsorption kinetics and thermodynamic studies of the batch adsorption process were used to examine the fundamental adsorption properties of phenol (P) and p-chlorophenol (PCP). The experimental equilibrium adsorption data were analyzed by three widely used two-parameters Langmuir, Freundlich and Dubinin-Radushkevich isotherms. The maximum P and PCP adsorption capacities based on the Langmuir isotherm were calculated at 56.818, 78.741, 92.593, 80.002, 103.579 and 131.579 mg/g for P and PCP onto ALO, AlO-AM and AlO-AP, respectively. The experimental kinetic data were analyzed by using Pseudo-first order and pseudo-second order kinetic models. A comparison of the kinetic models on the overall adsorption rate showed that the adsorption system can be best described by the pseudo-second order kinetics. Based on the calculated thermodynamic parameters such as enthalpy ($\Delta H°$), entropy ($\Delta S°$) and Gibb's free energy changes ($\Delta G°$). The negative $\Delta G°$ and $\Delta H°$ values indicated that the adsorption of P and PCP by AlO-AM and AlO-AP adsorbent was feasible, spontaneous and the process was exothermic in nature.

Keywords: Adsorption; Grafting alumina; Particle size; Isotherms; Phenols

1. Introduction

Water pollution is indeed of great concern since it is a major carrier of both organic and inorganic contaminants. Phenol and particularly chlorinated phenolic compounds are toxic to many aquatic organisms and cause unpleasant taste and odor to drinking water and can exert negative effect on different biological processes [1–3]. Due to their toxicity and adverse effect upon human and biota, the recommendation of World Health Organization (WHO), the permissible concentration of phenolic contents in potable waters is 1 μg/L [4] and the regulations by the Environmental Protection Agency, call for lowering phenol content in wastewaters is less than 1 mg/L [5]. Therefore, removal of phenols from waters and wastewaters is an important issue in order to protect public health and environment.

Alumina is abundant in many areas of the world and has unique physicochemical characteristics. The application of Al_2O_3 to remove phenols from wastewater has been reported [6–10]. High surface area, good porosity and thermal stability

* Corresponding author.

of alumina can make it an economical alternative adsorbent material for wastewater treatment. In recent years, polymeric adsorbent has been increasingly regarded as an alternative to the traditional adsorbent such as activated carbon and mineral clays for efficient removal of phenols from waste water for its good properties and mechanical intensity. The attention has been paid to the polymeric adsorbents could be attributed for its unique adsorption properties resulting from its high surface area, high volume of microspores and broad range of surface functional groups introduced in their consequent synthetic reaction [11–17].

In continuation of our earlier research concerning the removal of phenol and phenol derivatives from wastewater [18–23], in this study, two new monomer (AlO-AM) and polymer (AlO-AP) were synthesized, characterized, and investigated for the removal of P and PCP from aqueous solutions. The effects of experimental parameters such as contact time and temperature were studied. The adsorption mechanisms of P and PCP onto grafted aluminium oxide surfaces were evaluated in terms of thermodynamics and kinetics. The adsorption isotherms were described by using Langmuir, Freundlich, and D–R isotherms.

2. Experimental setup

2.1. Materials and measurements

Commercial puriss ≥98% aluminum oxide, anhydrous acrylic acid contains 200ppm MEHQ as inhibitor, 99% and anhydrous toluene, 99.8% were purchased from Sigma-Aldrich Chemical Company Inc. (Milwaukee, USA). The P and PCP used in the tests were also purchased from Sigma-Aldrich Chemical Company Inc. (Milwaukee, USA). Water used in all experiments was distilled and deionized.

Fourier-transform infrared (FTIR) measurements in the range of 500–4,000 cm^{-1} were obtained by using potassium bromide disc on Shimadzu model FTIR-8400S spectrophotometer (Japan). Differential scanning calorimetry (DSC) measurements were conducted with TA instruments Q1000 DSC, Ramp rate: 10°C/min under nitrogen atmosphere. Temperature and heat flow calibrated with standard indium of purity >99.99%. The thermal stabilities of AlO-AM and AlO-AP samples were investigated by thermogravemetric analyzer (TGA) (Netzsch STA 409 PG/PC thermogravimetricl analyzer, Selb Bavaria, Germany). Particle size distribution for AlO, AlO-AM and AlO-AP were made using Shimadzu, Sald-2101-Weal: V1.21 [24]. Quantitative analysis of P and PCP in aqueous solutions was carried out by a UV-Cary 100 Varian spectrophotometer (England).

2.2. Preparation of alumina-graft acrylic acid monomer (AlO-AM)

AlO-AM was prepared by the reaction between alumina and acrylic acid monomer in dry toluene (Fig. 1): Alumina (10.20 g, 0.10 mol) was weighed and placed in one-neck round bottom flask, followed by addition of 30 mL dry toluene. The monomer acrylic acid (25.20 g, 0.35 mol) was added dropwise to the standard solution of Alumina-toluene at room temperature, and then the mixture was agitating manually and ultrasonically for at least 3 h [25,26]. The product was filtered and washed with 20 mL distilled water, then 20 mL of acetone. The solid product was left to dry at room temperature.

2.3. Preparation of polymers by free radical polymerization

This polymer was synthesized by extension of alumina-graft acrylic acid monomer chain with new acrylic acid monomer according to Fig. 2 [27]. A two neck round-bottom flask contains 20 mL of dry toluene and 5.00 g of alumina-graft acrylic acid monomer which were placed in controlled water bath at 75°C ± 2°C under nitrogen atmosphere [28]. After 5 min benzoyl peroxide (0.10 g, 0.04 mmol) was added followed by addition of acrylic acid monomer (10.00 g, 0.14 mol) with stirring for 1 h. The product was filtered and washed first with 15 mL of toluene and with 15 mL of acetone, then left to dry at room temperature. The solid polymer was dried at 80°C for 12 h under vacuum to leave (80%) of AlO-AP.

2.4. Adsorption experiments

The stock solution of P and PCP (500 mg/L) was prepared. These solutions were prepared in 0.01 M NaCl in order to promote the flocculation and to have a constant background electrolyte concentration. The adsorption experiments were performed at 25°C, pH 6.5, using 0.2 g adsorbent added at 50 mL solution of P and PCP with different concentrations of 100–250 mg/L. All experiments were performed at a shaking speed of 200 rpm for 24 h to ensure the equilibrium of the adsorption process. After the contact time, the solids phases were centrifuged, and the supernatant was subsequently analyzed for the equilibrium concentration of P and PCP using a UV spectrophotometer at a wavelengths 270 and 280 nm for P and PCP, respectively. All experiments were run in triplicate to ensure reproducibility.

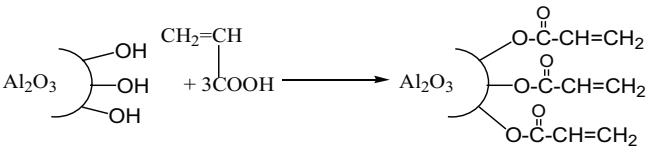

Fig. 1. The synthetic routes of AlO-AM.

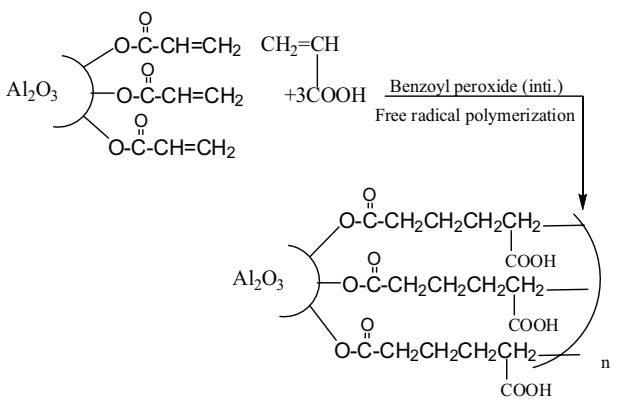

Fig. 2. The synthetic routes of AlO-AP.

The total amount of P and PCP retained by the solid phases was obtained by mass-balance equation:

$$q_e = \frac{\left(C_i - C_{\text{eq}}\right)V}{m} \quad (1)$$

where q_e is the quantity of the P or PCP in mg held by 1 g of the adsorbent; C_i is the initial concentration (mg/ L); C_{eq} is the equilibrium concentration (mg/ L) of the phenols in the aqueous phase; V is the volume of solution (L) and m is the mass of the adsorbent (g).

The effect of temperature on adsorption equilibrium was studied at temperatures 25°C, 40°C and 55°C, overnight. Kinetic studies were carried out for 50 mL working solution at constant pH 6.5 with initial concentration (175 mg/L) and the adsorbent dose of 0.2 g at 25°C.

2.5. Statistical analysis

To identify the best-fit model for the adsorption equilibrium and kinetic studies, this is a non-linear technique used to compare the data from the experiment and model predicted data as given in relation to q_e in the following equation [29]:

$$\text{MPSD} = 100\sqrt{\frac{1}{N-P}\sum_{i=1}^{n}\left(\frac{q_{e(\text{exp})} - q_{e(\text{pred})}}{q_{e(\text{exp})}}\right)^2 i} \quad (2)$$

where N is the number of experimental data points, P stands for number of parameters in the model, $q_{e(\text{exp})}$ and $q_{e(\text{pred})}$ are experimental and predicted uptake equilibrium and rates, respectively.

3. Results and discussion

3.1. Characterization of adsorbents

The structure of AlO-AM and AlO-AP was studied by FTIR spectroscopy, DSC. Thermal analysis (TG) and particle size distribution.

The FTIR spectra recorded for AlO, AlO-AM, AlO-AP and polyacrylic acid is shown in Fig. 1S. The spectra of pure Al_2O_3 (Fig. 1Sc) shows the large and intense two bands between 1,100 and 400 cm^{-1} are characteristics of Al-O vibrations in O-Al-O and Al-O-Al of pure alumina. The FTIR spectrum of AlO-AM (Fig. 1S(a)) showed an intense peak, associated with C = O stretching appears at 1,728 cm^{-1}. The broad band at 3,487 cm^{-1} is due to stretching of –OH groups of AlO-AM. The characteristic absorption bands of AlO-AP (Fig. 1S(b)) showed appearance the band at 2,858–2,925 cm^{-1} is due to aliphatic $\upsilon_{C\text{-}H}$ stretching. It also shows the band at 1,712 cm^{-1} due to C = O stretching. The appearance of the broad band at 3,180 to 4,215 cm^{-1} which is attributed to $\upsilon_{O\text{-}H}$ stretching of the carboxylic acid and disappearing of the two bands at 627 and 733 cm^{-1}, initially attributed to Al-O in Al_2O_3 confirming the formation of AlO-AP structure [6].

The DSC thermogram of AlO-AM (Fig. 2S) shows two endothermic peaks. The first big one centered at 215°C could be representing the melting or degradation of grafted monomer followed by the small one at 251°C. The later could be arises from the melting of high molecular weight chains. Normally, the melting endothermic peak accompanying with high value of enthalpy (46.46 J/g) compared with the other one. The DSC thermogram of AlO-AP (Fig. 2S) showed two peaks, exo- and endothermic. The first exothermic peak centered at 223°C could be attributed to the crystallization transition temperature. This resulted semi crystalline polymers with crystals of different sizes and orientation. Thus, the crystallization temperature brought about crystals to the same sizes and perfection. The second endothermic peak at 286°C which is almost the half way of the grafted monomer appear as overlapping peaks representing the melting of the entire polydispers polymer. The enthalpy of melting is also high compared with crystallization exothermic value.

The thermal stability of AlO-AM and AlO-AP was measured by thermogravemetry using TG and differential thermogravimetric analysis (DTG) instruments under N_2 gas atmosphere with heating rate 10°C/min (Fig. 3S). The general features of TG thermograms showing the weight loss trace of two distinguishable maxima. The first one centered at 210°C and 220°C with average percentage weight loss 18.7 and 11.5% and the second peak centered at 450°C and 470°C with average percentage weight loss 10.2% and 3.5% for AlO-AM and AlO-AP, respectively.

The particle size has a great importance because it affects most of the properties such as density of compact, porosity, dimensional stability, agglomerations, flow, and mixing characteristics. Particle size distribution is the statistical relation between amount and size. Size distribution is based on the percentage by weight of sample powder which is retained on a screen of given mesh size from a given weight of starting material after passing through the just coarsen sieve. For example, "25% minus 100 plus 150" means that 25% (by weight) of the particles pass the 100 mesh-screen but are retained by the 150 mesh screen. The results of particle size distribution measurement for AlO, AlO-AM and AlO-AP (Fig. 4S) are listed in Table 1. The results indicate a small different in particle size distribution to AlO-AM, but there is a large different in distribution to grafted AlO-AP polymer. The differences in particle size distribution on the percentage by weight of sample indicate that the synthesized monomer (AlO-AM) and the polymer (AlO-AP) were successful. This can be considering as another proof for the grafting process including AlO-AM and the polymerization to produce polymer (AlO-AP).

3.2. Effect of contact time

Fig. 3 illustrates the influence of contact time on the P and PCP uptake on AlO, AlO-AM and AlO-AP adsorbents at 175 mg/L initial concentration and the contact time range of 5–120 min. It can be seen that the remaining concentration of

Table 1
The percentage of particle size distribution

Adsorbent	25% D	50% D	75% D	Mean value
AlO	6.925	11.799	18.177	10.377
AlO-AM	6.846	11.928	18.900	11.143
AlO-AP	7.574	14.40	27.131	14.295

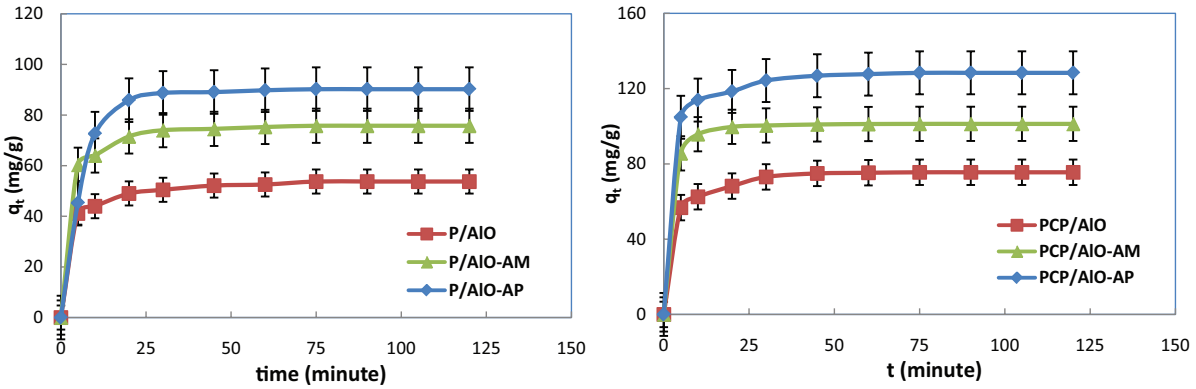

Fig. 3. Effect of contact time on the adsorption of P and PCP onto AlO, AlO-AM and AlO-AP; Initial P and PCP concentration 175 mg/ L; pH = 6.5; temperature 25°C.

P and PCP becomes asymptotic to the time axis after 75 min. It also seen that both the P and PCP adsorption onto these adsorbents is very fast in the first 25 min then it becomes slower near the equilibrium. This can be attributed to the large number of vacant surface sites available for adsorption at the initial stage which in time becomes difficult to be occupied as a result of repulsive forces between the solute molecules on the solid and bulk phases [30]. These results regarding the time to reach equilibrium are in accordance with the literature data [11,30,31].

3.3. Adsorption isotherms

The experimental data were fitted with Langmuir, Freundlich and Dubinin-Radushkevich (D-R). Adsorption isotherms of P and PCP have been established at three different temperatures: 25°C, 35°C, and 45°C.

Langmuir adsorption isotherm [32] applied to equilibrium adsorption assuming a mono-layer adsorption onto the surface of the adsorbent with a finite number of identical sites. This isotherm can be represented by the following relationship:

$$\frac{C_{eq}}{q_e} = \frac{1}{q_{max} K_L} + \frac{C_{eq}}{q_{max}} \tag{3}$$

where q_e is the uptake of P and PCP per unit weight of the adsorbent (mg/g), q_{max} is the maximum P and PCP uptake (mg/g K_L is the Langmuir constant (L/mg) and related to the energy of adsorption and C_{eq} is the equilibrium (residual) concentration of P and PCP (mg/L).

The influence of the adsorption isotherm shape can be discussed to examine whether adsorption is favorable in terms of R_L, a dimensionless constant referred to as separation factor or equilibrium parameter. R_L is defined by the following relationship:

$$R_L = \frac{1}{(1 + K_L C_i)} \tag{4}$$

where C_i is the initial concentration for P and PCP (mg/L).

R_L values between 0 and 1 indicate favorable adsorption, while $R_L > 1$, $R_L = 1$, and $R_L = 0$ indicate unfavorable, linear, and irreversible adsorption isotherms, respectively [33].

A plot of C_{eq}/q_e vs C_{eq} gives straight line as shown in Fig. 4. q_{max} and K_L were determined from slope and intercept of the plot (Tables 2 and 3). It is clear from Tables 2 and 3 that all R_L values lie between 0 and 1 indicating the favorable adsorption of P and PCP by AlO, AlO-AM and AlO-AP.

Comparison of the q_{max} values of phenol and phenol derivatives with other alumina and modified alumina adsorbents reported in the literature [6,8,9,34,35] is listed in Table 4. The q_{max} of phenol onto AlO-AM and AlO-AP has a high value among listed adsorbents considering this result indicates that AlO-AM and AlOAP have a significant potential for removal of phenols from aqueous solutions.

The Freundlich isotherm based for adsorption on a heterogeneous surface. The linearized form of Freundlich adsorption isotherm is [36]:

$$\log q_e = \log K_F + \frac{1}{n} \log C_{eq} \tag{5}$$

where K_F (mg/ g) is the constant related to the adsorption capacity and n is the empirical parameter related to the intensity of adsorption. The value of n varies with the heterogeneity of the adsorbent and for favorable adsorption process the value of n should be less than 10 and higher than unity [37]. The values of K_F and $1/n$ are determined from the intercept and slope of linear plot of ln q_e versus lnC_{eq}, respectively (Fig. 5). All the n values obtained from the Freundlich model are greater than unity at all solution temperatures, indicating that adsorption of P and PCP onto AlO, AlO-AM and AlO-AP was favorable (Tables 2 and 3).

D-R model adsorption is commonly used to describe the adsorption isotherm of single solute system, although this is analogue to Langmuir model, D-R model is more general than Langmuir as it rejects the homogenous surface or constant adsorption potential [38]. The linearized equation of D-R isotherm model is:

$$\ln q_e = \ln q_{max} - \beta\varepsilon^2 \tag{6}$$

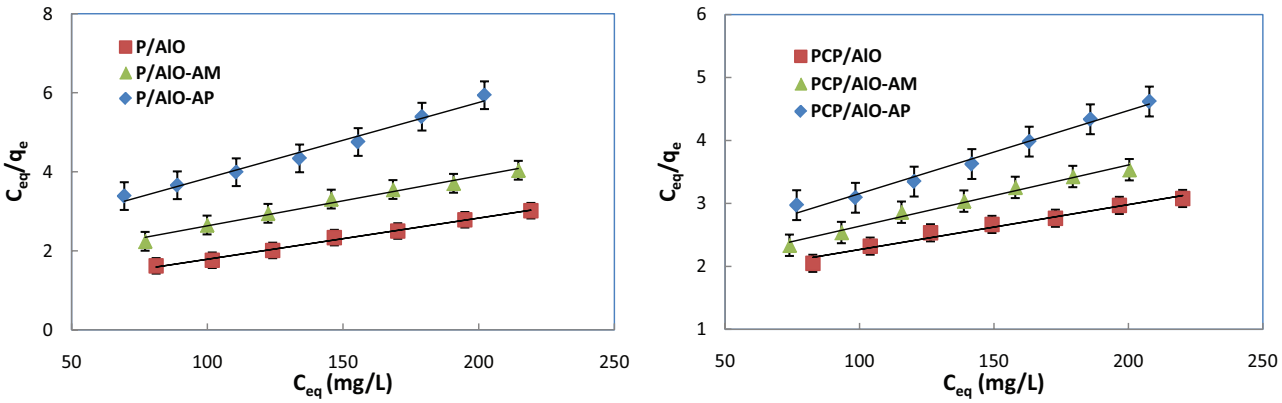

Fig. 4. The Langmuir isotherm plot of adsorption of P and PCP onto AlO, AlO-AM and AlO-AP; pH 6.5; at temperature 25°C.

Table 2
Constants parameters and correlation coefficients calculated for various adsorption isotherm models at different temperatures for P on AlO, AlO-AM and AlO-AP

Adsorbate	P/AlO			P/AlO-AM			P/AlO-AP		
T/°C	25°C	35°C	45°C	25°C	35°C	45°C	25°C	35°C	45°C
Langmuir									
q_{max} (mg/g)	56.818	52.632	47.619	78.741	70.423	64.103	92.593	86.957	67.568
K_L (L/mg)	0.009	0.005	0.008	0.009	0.006	0.005	0.013	0.009	0.006
R_L	0.303	0.316	0.425	0.301	0.414	0.392	0.237	0.316	0.419
R^2	0.9851	0.9875	0.9866	0.9867	0.9638	0.9917	0.9964	0.9825	0.8924
MPSD	1.978	0.603	2.010	0.549	0.716	0.540	0.197	0.601	2.826
Freundlich									
K_F (L/g)	8.188	2.161	1.984	5.097	1.712	3.137	8.188	5.003	2.125
N	2.506	1.571	1.307	2.291	1.709	2.069	2.506	2.205	1.885
R^2	0.9757	0.9801	0.9761	0.9932	0.9647	0.9721	0.9657	0.9547	0.9853
MPSD	2.066	0.536	0.646	0.381	1.094	0.750	1.062	1.437	0.561
D-R									
q_{max} (mg/g)	48.293	31.147	23.901	63.059	41.104	39.837	78.293	57.271	41.104
E (kJ/mol)	1.236	1.529	1.327	1.523	1.133	1.529	1.736	2.033	2.122
R^2	0.9692	0.9898	0.9454	0.8864	0.9636	0.9529	0.9385	0.8707	0.8871
MPSD	1.229	1.853	2.556	1.745	0.301	0.487	0.107	1.405	1.245

where q_{max} is the D-R monolayer capacity (mg/g), β is a constant related to adsorption energy (mol²/kJ²), and ε is the Polanyi potential which is related to the equilibrium concentration as follows [39]:

$$\varepsilon = RT\ln\left(1+\frac{1}{C_{eq}}\right) \tag{7}$$

where R is gas constant (8.314 J/mol K), T is temperature (K).

The adsorption free energy E (kJ/ mol) is defined as the free energy change required for transferring one mole of adsorbate from infinity in the solution to solid surface, this energy is calculated as follows:

$$E = \frac{1}{\sqrt{2\beta}} \tag{8}$$

A plot of $\ln q_e$ vs. ε^2 is given in Fig. 6. Adsorption capacities q_{max} and the main sorption energies E are calculated for the P and PCP removed from the aqueous phase by the AlO, AlO-AM and AlO-AP are listed in Tables 2 and 3. The value of E is used to differentiate the physisorption or chemisorption of P and PCP on the adsorbent surfaces; the values of E calculated using Eq. (7) are shown in Tables 2 and 3 and range in between 1.126 and 2.122 kJ/mol. If the magnitude of E is between 8 and 16 kJ/mol, the adsorption process proceeds by ion-exchange or chemisorption [40], while for values of E < 8 kJ/mol, the adsorption process is of a physical nature [41]. Therefore, the data would indicate that the adsorption process of P and PCP onto AlO, AlO-AM and AlO-AP is physisorption.

The characteristics of ions, molecules (shape, size, charge, etc) present in wastewater and their concentration have profound influence on the extent of adsorption. As shown in Tables 2 and 3, the adsorption capacity for PCP is

Table 3
Constants parameters and correlation coefficients calculated for various adsorption isotherm models at different temperatures for PCP on AlO, AlO-AM and AlO-AP

Adsorbate	PCP/AlO			PCP/AlO-AM			PCP/AlO-AP		
T/°C	25°C	35°C	45°C	25°C	35°C	45°C	25°C	35°C	45°C
Langmuir									
q_{max}(mg/g)	80.002	75.188	60.606	103.093	93.547	81.301	131.579	99.010	76.336
K_L(L/mg)	0.007	0.010	0.013	0.006	0.003	0.005	0.008	0.007	0.005
R_L	0.369	0.284	0.229	0.407	0.598	0.448	0.450	0.423	0.457
R^2	0.9889	0.9899	0.9944	0.9872	0.8663	0.8926	0.9781	0.9881	0.9201
MPSD	2.591	2.018	1.054	1.501	2.870	1.776	1.347	1.023	2.235
Freundlich									
K_F(L/g)	2.693	5.011	5.703	2.361	1.311	1.237	2.93	2.494	1.708
n	1.659	2.291	2.565	1.629	1.376	1.519	1.835	1.746	1.722
R^2	0.9966	0.9757	0.9621	0.9744	0.9764	0.9841	0.9962	0.9974	0.9779
MPSD	1.060	1.530	2.062	2.631	1.791	1.029	1.544	1.018	1.652
D-R									
q_{max}(mg/g)	76.769	52.326	44.492	89.004	43.406	39.516	121.769	84.179	57.409
E(kJ/mol)	1.328	1.834	2.041	1.527	1.225	1.126	1.528	2.068	1.934
R^2	0.9553	0.97286	0.9704	0.9827	0.9875	0.9509	0.9845	0.9802	0.9768
MPSD	2.234	1.026	1.262	1.255	1.061	1.712	1.003	1.012	1.166

Table 4
Comparison of maximum adsorption capacity (q_{max}, mg/g) for phenol and phenol derivatives by alumina and modified alumina adsorbents.

Adsorbent	Adsorbate	Condition		q_{max}/mg/g	Reference
		pH	T/°C		
Al_2O_3/HDTMA[a]	Nitrophenol	6.0	25	9.251	[6]
Synthetic alumina	Phenol	6.5	25	3.149	[34]
CNT- Al_2O_3	Phenol	6.0	25	2.778	[8]
	Chlorophenol	6.0	25	3.679	
ACs- Al_2O_3	Phenol	7.0	25	3.456	[35]
FA- Al_2O_3	Phenol	7.0	25	2.105	[9]
AlO-AM	Phenol	6.5	25	78.741	This work
	Chlorophenol	6.5	25	103.093	
AlO-AP	Phenol	6.5	25	92.593	This work
	Chlorophenol	6.5	25	131.579	

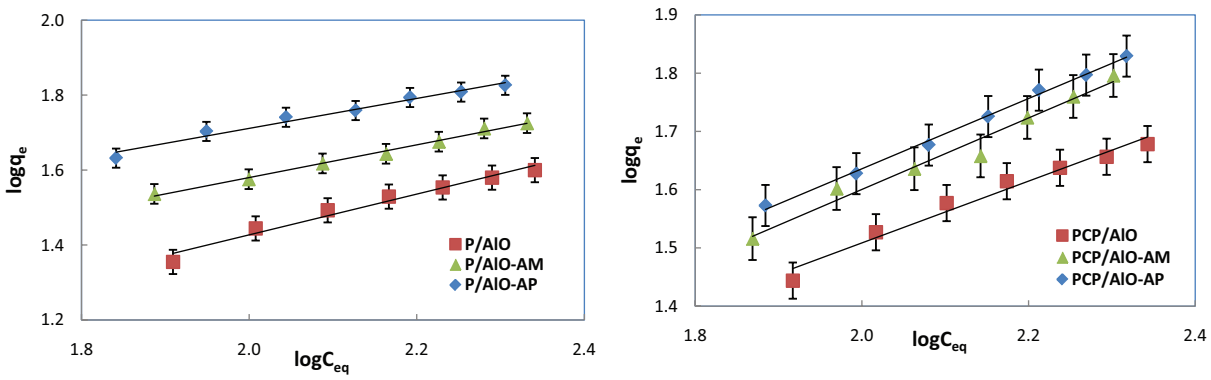

Fig. 5. The Freundlich isotherm plot of P and PCP onto AlO, AlO-AM and AlO-AP; pH 6.5; temperature 25°C.

greater than for *P* on each of the sample tested, explained by the lower solubility and pKa value of PCP compared with *P*. Such a sequence shows clearly the greater adsorption for the more acidic phenols, that is P and PCP with pK_a 9.99 and 9.43.

The Langmuir, Freundlich and D-R isotherm constants at different temperatures for the adsorption of P and PCP on AlO, AlO-AM and AlO-AP alongside with the R^2 and MPSD values are presented in Tables 2 and 3 respectively. Jaynes and Boyd [42] proposed that the adsorption conforms to the Langmuir, Freundlich and D-R models when the value of correlation coefficient (R^2) is greater than 0.89. The R^2 values shown in Tables 2 and 3 are greater than 0.89 and the low MPSD values (0.301 to 2.826) for the three models indicating that these three isotherm models can adequately describe the adsorption data. The applicability of the three isotherm models to the all investigated systems implies that both monolayer adsorption and heterogeneous surface conditions exist under the experimental conditions studied. The adsorption of P and PCP on these surfaces is thus complex, involving more than one mechanism. Similar observations have been previously for the adsorption of phenols by other adsorbents [18,23].

From the values of the maximum adsorption capacity, q_{max}, given in Tables 2 and 3, it can be concluded that the capacity of adsorption of P and PCP by the studied three surfaces follows the sequence, AlO-AP > AlO-AM > AlO. This could be attributed to the fact that AlO-AP has functionalized with more carboxylic acid groups which have a good affinity for the formation of hydrogen bonding with the hydroxyl groups of P and PCP. Similar results have been reported by other researchers [11,13,32,36,43].

3.4. Adsorption kinetic

The adsorption kinetic is one of the most important data in order to understand the mechanism of the adsorption and to assess the performance of the adsorbents. Two kinetic models including the pseudo-first order of Lagergren and pseudo-second order models were applied for the experimental data to predict the adsorption kinetic.

The linearized form of the pseudo-first order rate equation can be written as [44]:

$$\ln\left(q_e - q_t\right) = -K_1 t + \ln q_e \tag{9}$$

where q_t (mg/g) is the amount of absorbed at time t (min) and k_1 (min^{-1}) is the rate constant for pseudo-first-order model. A straight line of $\ln(q_e - q_t)$ vs t (Fig. 7) suggests the applicability of this kinetic model, and q_e and k_1 can be determined from the intercept and slope of the plot, respectively.

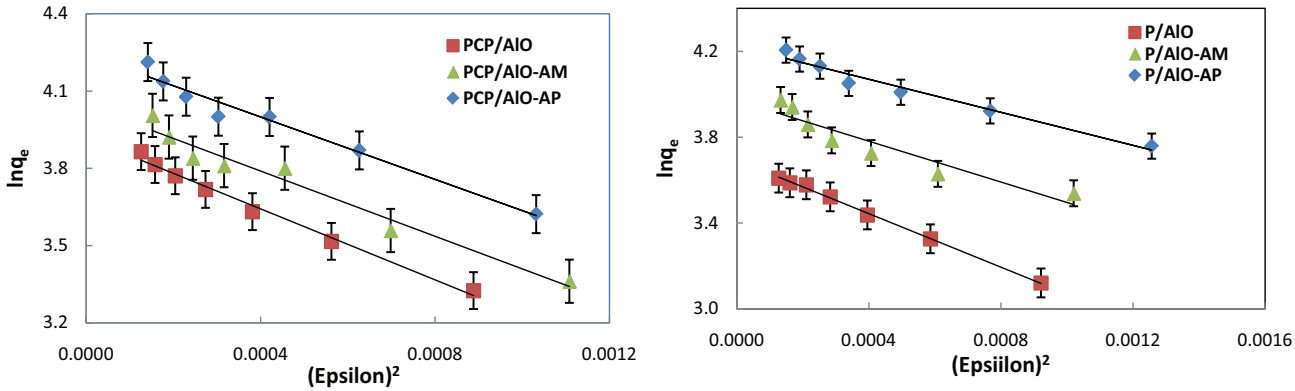

Fig. 6. The D-R isotherm plot of P and PCP onto AlO, AlO-AM and AlO-AP; pH 6.5; temperature 25°C.

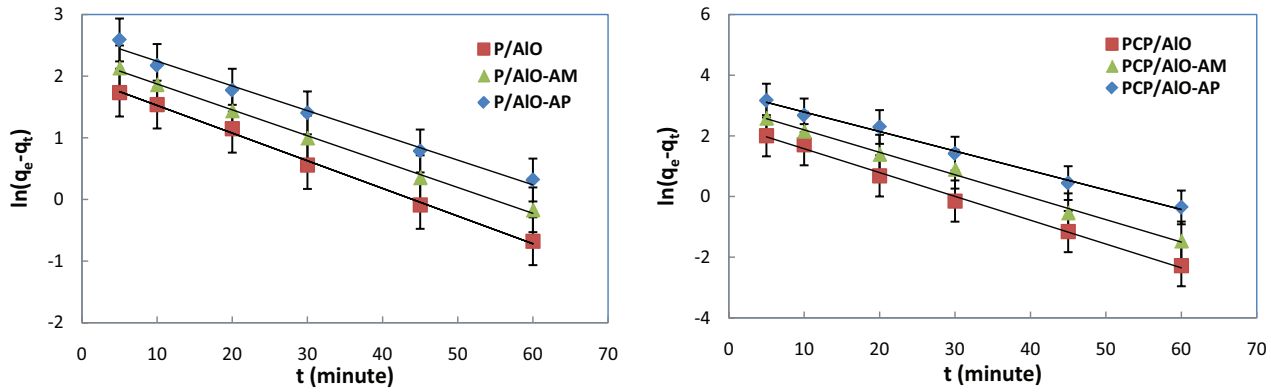

Fig. 7. Pseudo-first-order kinetics of adsorption of P and PCP onto AlO, AlO-AM and AlO-AP. Initial P and PCP concentration 175 mg/ L; pH 6.5; temperature 25°C.

Experimental data was further analyzed by using the pseudo-second order kinetic equation [45]:

$$\frac{t}{q_t} = \frac{1}{K_2 q_e^2} + \frac{t}{q_e} \tag{10}$$

where k_2 is the rate constant of pseudo-second-order model in (g/mg.min). A plot of t/q_t vs t, give the slope =1/q_t and intercept = $1/q_e^2 k_2$ (Fig. 8).

The results of the kinetic parameters are summarized in Table 5 alongside with the R^2 and MPSD values. It can be seen that the calculated coefficient of determination (R^2) is very close to unity in comparison with pseudo-first order model. Also, for the pseudo-second order model; the low MPSD values (0.182–0.624) and that $q_{e.Calcd.}$ values agree with the experimental values indicate that the pseudo-second order kinetic model provided a good correlation for the adsorption of P and PCP onto AlO, AlO-AM and AlO-AP comparing to the pseudo-first order model.

3.5. Thermodynamic parameters

The free energy change of the specific adsorption $\Delta G°$ is linked to the distribution coefficient $K_{d,}$ through the following equation:

$$\Delta G^{\circ} = -RT \ln K_d \tag{11}$$

The distribution coefficient (K_d) of P and PCP between the aqueous phase and the solid phase can be directly obtained using [39]:

$$K_d = \frac{q_e}{C_{eq}} \tag{12}$$

K_d values was obtained from the intercept of the plot of $\ln q_e/C_{eq}$ vs. q_e.

The relationship between $\ln K_d$ and temperature (T) is expressed using the following equations [46]:

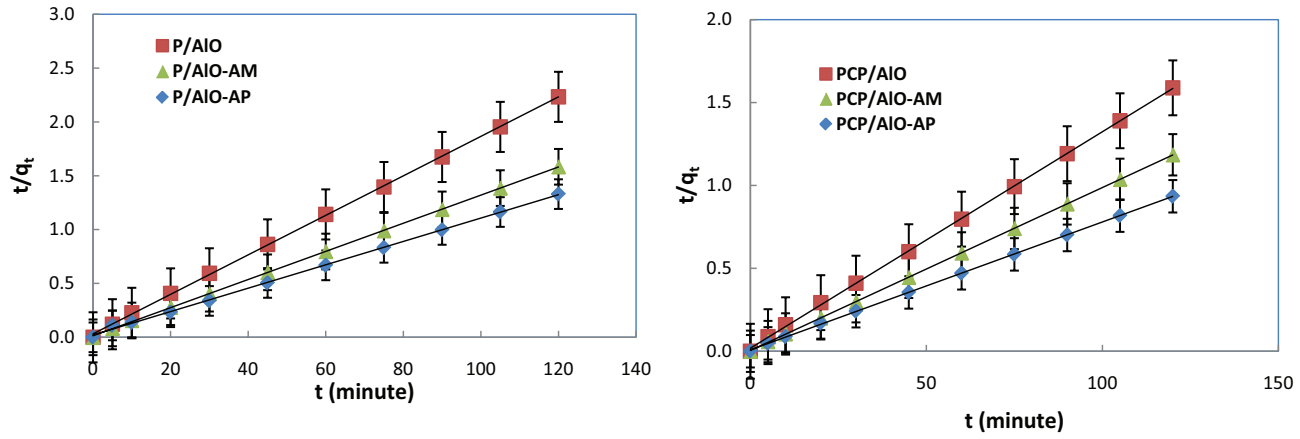

Fig. 8. Pseudo-second-order kinetics of adsorption of P and PCP onto AlO, AlO-AM and AlO-AP. Initial P and PCP concentration 175 mg/ L; pH 6.5; temperature 25°C.

Table 5
Pseudo-first order and pseudo-second order adsorption rate constant and calculated $q_{e.Clcd.}$ and experimental $q_{e.Exp.}$ values for the adsorption of P and PCP on AlO, AlO-AM and AlO-AP

$q_{e.Exp.}$ (mg/g)	Pseudo-first order				Pseudo-second order			
	k_1 (min^{-1})	$q_{e.Clcd.}$ (mg/g)	R^2	MPSD	K_2 (g/mg.min)	$q_{e.Clcd.}$ (mg/g))	R^2	MPSD
P/AlO								
56.818	0.044	13.706	0.9398	29.703	0.011	54.645	0.9997	0.433
P/AlO-AM								
78.741	0.063	18.047	0.9135	28.423	0.012	76.336	0.9999	0.283
P/AlO-AP								
92.593	0.079	34.661	0.9737	27.141	0.006	91.743	0.9991	0.624
PCP/AlO								
80.002	0.083	30.661	0.9112	29.107	0.009	76.336	0.9998	0.397
PCP/AlO-AM								
103.093	0.086	14.127	0.9411	26.973	0.003	102.041	1.0000	0.182
PCP/AlO-AP								
131.579	0.065	30.135	0.9837	26.474	0.007	129.870	0.9999	0.254

Table 6
Thermodynamic parameters for the adsorption of P and PCP on AlO, AlO-AM and AlO-AP

T/°C	ΔG kJ/mol	ΔH kJ/mol	ΔS kJ/K.mol
	P/AlO		
25°C	–7.811	–29.545	–73.163
40°C	–6.985		
55°C	–5.615		
	P/AlO-AM		
25°C	–7.407	–30.289	–76.929
40°C	–6.084		
55°C	–5.107		
	P/AlO-AP		
25°C	–6.462	–37.719	–104.515
40°C	–5.202		
55°C	–3.307		
	PCP/AlO		
25°C	–6.115	–35.019	–96.426
40°C	–5.171		
55°C	–3.189		
	PCP/AlO-AM		
25°C	–7.640	–21.990	–47.631
40°C	–7.402		
55°C	–6.179		
	PCP/AlO-AP		
25°C	–6.606	–34.419	–93.325
40°C	–5.174		
55°C	–3.8.9		

$$\Delta G^{\circ} = \Delta H^{\circ} - \mathrm{T}\Delta S^{\circ} \tag{13}$$

$$\ln K_d = -\frac{\Delta H^{\circ}}{RT} + \frac{\Delta S^{\circ}}{R} \tag{14}$$

where $\Delta H°$ is the change in enthalpy (kJ/mol), $\Delta S°$ is the change in entropy (J/mol K). From equation (14) the values of $\Delta H°$ and $\Delta S°$ can be calculated from the slope and intercept of the linear variation of $\ln K_d$ with reciprocal temperature (Fig. is not shown). The values of $\Delta G°$,$\Delta H°$, and $\Delta S°$ for adsorption of P and PCP onto AlO, AlO-AM and AlO-AP are given in Table 6.

The negative value of the Gibbs free energy change $\Delta G°$ indicated that the spontaneous nature of adsorption for P and PCP by AlO, AlO-AM and AlO-AP. Enhancement of the adsorption capacity at higher temperatures may be attributed to the enlargement of pore size of the adsorbent surface [47]. The change of free energy for physisorption is between −20 and 0 kJ/ mol, but chemisorptions are at the range from −80 to −400 kJ/mol [48]. Hence, P and PCP adsorption was physical in nature. The negative value of enthalpy change $\Delta H°$ shows that adsorption of P and PCP onto AlO, AlO-AM and AlO-AP to be exothermic in nature. Whereas the negative values of $\Delta S°$ suggested a decrease in randomness at the solid/solution interface during the adsorption.

4. Conclusions

AlO-AM and AlO-AP were synthesized by grafting commercial AlO and have been characterized by a FTIR, DSC, TGA and particle size distribution confirming that acrylic acid monomer and poly(acrylic acid) has been grafted onto AlO backbone. The equilibrium data were described by the Langmuir, Freundlich and D-R. The monolayer sorption capacity obtained from Langmuir model was found to be 56.818, 78.741, 92.593, 80.002, 103.579 and 131.579 mg/g for P and PCP onto AlO, AlO-AM, and AlO-AP, respectively. The kinetics studies demonstrated that the adsorption of P and PCP onto AlO, AlO-AM and AlO-AP adsorbents followed the pseudo-second order model. The calculated change in free energy $\Delta G°$ and enthalpy $\Delta H°$ indicated that the adsorption process was spontaneous and exothermic in nature. The negative value of $\Delta S°$ shows the decreased randomness of the solid/solution interfaces during the adsorption of P and PCP on AlO, AlO-AM and AlO-AP.

References

[1] M. Sobiesiak, B. Podkoscielna, Preparation and characterization of porous DVB copolymers and their applicability for adsorption (solid-phase extraction) of phenol compounds, Appl. Surf. Sci., 257 (2010) 1222–1227.
[2] Z. Ioannou, J. Simitzis, Adsorption kinetics of phenol and 3-nitrophenol from aqueous solutions on conventional and novel carbons, J. Hazar. Mater., 171 (2009) 954–964.
[3] F.A. Banat, V. Al-Bashir, S. Al-Asheh, O. Hayajneh, Adsorption of phenol by bentonite, Environ. Pollution, 107 (2000) 391–398.
[4] WHO (World Health Organization), Guidelines for Drinking-water Quality: first addendum to the Fourth Edition, Health criteria and supporting information, Geneva, Switzerland, 2017.
[5] N.N. Dutta, S. Brothakur, R. Baruaha, A novel process for recovery of phenol from alkaline wastewater: laboratory study and predesigned cost estimate, Water Environ. Res., 70 (1998) 4–9.
[6] M. Aazza, H. Ahlafi, H. Moussout, H. Maghat, Ortho-nitro-Phenol adsorption onto alumina and surfactant modified alumina: kinetic, isotherm and mechanism, J. Environ. Chem. Eng., 5(4) (2017) 3418–3428.
[7] I.C. Yeh, J.L. Lenhart, B.C. Rinderspacher, Molecular dynamics simulations of adsorption of catechol and related phenolic compounds to alumina surfaces, J. Phys. Chem., C119(14) (2015) 7721–7731.
[8] Ihsanullah, H.A. Asmaly, T.A. Saleh, T. Laoui, V.K. Gupta, M.A. Atieh, Enhanced adsorption of phenols from liquids by aluminum oxide/carbon nanotubes: comprehensive study from synthesis to surface properties, J. Mol. Liq., 206 (2015) 176–182.
[9] H.A. Asmaly, Ihsanullah, A. Abussaud, T.A. Saleh, T. Laoui, V.K. Gupta, M.A. Atieh, Adsorption of phenol on aluminum oxide impregnated fly ash, Desal. Wat. Treat., 57 (2016) 6801–6808.
[10] T.G. Danis, T.A. Albanis, D.E. Petrakis, P.J. Pomonis, Removal of chlorinated phenols from aqueous solutions by adsorption on alumina pillared clays and mesoporous alumina aluminum phosphates. Water Res., 32 (1998) 295–302.
[11] A.H. Al-Muhtase, K.A. Ibrahim, A.B. Albadarin, O. Ali-khashman, G.M. Walkerb, M.N.M. Ahmad, Remediation of phenol-contaminated water by adsorption using poly(methyl methacrylate) (PMMA), Chem. Eng. J., 168 (2011) 691–699.
[12] X. Zeng, Y. Fan, G. Wu, R. Shi, Enhanced adsorption of phenol from water by a novel polar post-crosslinked polymeric adsorbent, J. Hazard. Mater., 169 (2009) 1022–1028.
[13] J. Huang, Adsorption properties of a microporous and mesoporous hyper- crosslinked polymeric adsorbent functionalized with phenoxy groups for phenol in aqueous solution, J. Colloid Interface Sci., 339 (2009) 296–301.

[14] F. An, B. Gao, X. Feng, Adsorption mechanism and property of novel composite material PMAA/SiO2 towards phenol, Chem. Eng. J., 153 (2009) 108–113.
[15] N. Li, Z. Mei, X. Wei, Study on sorption of chlorophenols from aqueous solutions by an insoluble copolymer containing b-cyclodextrin and polyamido amine units, Chem. Eng. J., 192 (2012) 138–145.
[16] N. Li, Z. Mei, S.M. Chen, Removal of 4-chlorophenol from aqueous solutions by cyclodextrin polymer, Fresenius Environ. Bull., 18 (2009) 2249–2253.
[17] F. An, R. Du, X. Wang, M. Wan, X. Dai, J. Gao, Adsorption of phenolic compounds from aqueous solution using salicylic acid type adsorbent, J. Hazard. Mater., 201–202 (2012) 74–81.
[18] B. Ihaddadene, L. Tifouti1, A.H. Al-Dujaili, N. Gherraf, Enhancing batch adsorption capacity of bentonite, kaolinite and their organomodified forms for phenol removal, Int. J. Chem. Tech. Res., 8 (2015) 1749–1762.
[19] R.Z. Al- Bakaina, R.A. Abu-Zuraykb, I. Hamadneha, F.I. Khalilia, A.H. Al-Dujaili, A study on removal characteristics of o-, m-, and pnitrophenol from aqueous solutions by organically modified diatomaceous earth, Desal. Wat. Treat., 56 (2014) 826–838.
[20] O.E.A. Adam, A.H. Al-Dujaili, The Removal of phenol and Its derivatives from aqueous solutions by adsorption on petroleum asphaltene, J. Chem., ID 694029 (2013) 1–8.
[21] M.L. Sekirifa, S. Pallier, M. Hadj-Mahammed, D. Richard, L. Baameur, A.H. Al-Dujaili, Measurement of the performance of an agricultural residue-based activated carbon aiming at the removal of 4-chlophenol from aqueous solution, Energy Procedia, 36 (2013) 94–103.
[22] M.L. Sekirifa, M. Hadj-Mahammed, S. Pallier, L. Baameur, D. Richard, A.H. Al-Dujaili, Preparation and characterization of an activated carbon from a datestones variety by physical activation with carbon dioxide, J. Anal. Appl. Pyrolysis, 99 (2013) 155–160.
[23] U.F. Alkaram, A.A. Mukhalis, A.H. Al-Dujaili, The removal of phenol from aqueous solutions by adsorption using surfactant-modified bentonite and kaolinite, J. Hazard. Mater., 169 (2009) 324–332.
[24] A.K. Sinha, Powder Metallurgy. 2nd ed., Delhi, Karan Printing Service, 1987.
[25] A.A. Tsyganenko, P.P. Mardilovich, Structure of alumina surfaces. J. Chem. Soc., Faraday Trans., 92 (1996) 4843–4852.
[26] B.K. Hordern, Chemistry of alumina, reactions in aqueous solution and its application in water treatment, Adv. Colloid Interface Sci., 110 (2004) 19–48.
[27] B. Wang, Y.P. Wang, P. Zhou, Z.Q. Liu, S.Z. Luo, W. Chu, Z. Guo, Formation of poly(acrylic acid)/alumina composite via in situ polymerization of acrylic acid adsorbed within oxide pores, Colloids Surf A: Physicochem. Eng. Aspects, 514 (2016) 168–177.
[28] J. Brandrub, E.H. Immergut, E.A. Grulke, Editors, Handbook of Polymer, 4th ed., John Wiley, New York, 1999.
[29] Igberase, E. Osifo, P. Ofomaja, A. Adsorption of metal ions by microwave assisted grafting of cross-linked chitosan beads. Equilibrium, isotherm, thermodynamic and desorption studies, Appl. Organometal. Chem., e4131 (2017) 1–14.
[30] C. Pacurariu, G. Mihoc, A. Popa, S.G. Muntean, R. Ianos, Adsorption of phenol and p-chlorophenol from aqueous solutions on poly (styrene-co-divinylbenzene) functionalized materials, Chem. Eng. J., 222, (2013) 218–227.
[31] J. Huang, XJin, S. Deng, Phenol adsorption on an N-methylacetamide-modified hypercrosslinked resin from aqueous solutions, Chem. Eng. J., 192 (2011) 192– 200.
[32] I. Langmuir, The adsorption of gases on plane surface of glass, mica and platinum, J. Am. Chem. Soc., 40 (1918) 1361–1403.
[33] S. Renganathan, W.R. Thilagaraj, L.R. Miranda, P. Gautam, M. Velan, Accumulation of Acid Orange 7, Acid Red 18 and Reactive Black 5 by growing Schizophyllum communication, Bioresour. Technol., 97 (2006) 2189–2193.
[34] N. Salahudeen, A.S. Ahmed, A.H. Al-Muhtaseb, M. Dauda, S.M. Waziri, B.Y. Jibril, J. Al-Sabahi, Synthesis, characterization and adsorption study of nano-sized activated alumina synthesized from kaolin using novel method, Powder Technol., 280 (2015) 266–272.
[35] B. Abussaud, H.A. Asmaly Ihsanullah, T.A. Saleh, V.K. Gupta, T. Laoui, M.A. Atieh, Sorption of phenol from waters on activated carbon impregnated with iron oxide, aluminum oxide and titanium oxide, J. Mol. Liq., 213 (2016) 351–359.
[36] H.M.F. Freundlich, About the adsorption, Z. für Physikalische Chemie, 57 (1906) 385–470.
[37] H.B. Senturk, D. Ozdes, A. Gundogdu, C. Duran, M. Soylak, Removal of phenol from aqueous solutions by adsorption onto organomodified Tirebolu bentonite: equilibrium, kinetic and thermodynamic study, J. Hazard. Mater., 172 (2009) 353–362.
[38] M.M. Dubinin, E.D. Zaverina, L.V. Radushkevich, Sorption and structure of active carbon I. Adsorption of organic vapors, J. Phys. Chem. A, 21 (1947) 1351–1362.
[39] C. Kütahyalı, M. Eral, Sorption studies of uranium and thorium on activated carbon prepared from olive stones: kinetic and thermodynamic aspects, J. Nucl. Mater., 396 (2010) 251–256.
[40] Y.S. Ho, J.F. Porter, G. McKay, Equilibrium isotherm studies for the sorption of divalent metal ions onto peat: copper, nickel and lead single component systems, Water, Air Soil Pollut. 141 (2002) 1–5.
[41] M.S. Onyango, Y. Kojima, A. Kumar, D. Kuchar, Uptake of fluoride by Al3+ pretreated low-silica synthetic zeolites: adsorption equilibrium and rate studies, Sep. Sci. Technol., 41 (2006) 683–689.
[42] W.F. Jaynes, S.A. Boyd, Hydrrophobicity of siloxane surfaces in smectites as revealed by aromatic hydrocarbon adsorption from water, Clay Miner., 39 (1991) 428–436.
[43] D.K. Singh, B. Srivastva, Removal of phenol pollutant from aqueous solutions using various adsorbents, J. Sci. Indus. Res., 61 (2002) 208–218.
[44] S. Lagergren, About the theory of so-called adsorption of soluble substances, K Sven Vetensk akad Handl, 24 (1898) 1–39.
[45] Y.S. Ho, G. Mckay, A comparison of chemisorptions kinetic models applied to pollutant removal on various sorbents, Process Saf. Environ. Prot., 76 (1998) 332–340.
[46] S.S. Tahir, N. Rauf, Thermodynamic studies of Ni(II) sorption onto bentonite from aqueous solution, J. Chem. Thermodyn., 35 (2003) 2003–2009.
[47] M.K. Jha, R.R. Upadhyay, J.C. Lee, V. Kumar, Treatment of rayon waste effluent for the removal of Zn and Ca using Indion BSR resin, Desalination, 228 (2008) 97–107.
[48] F. Arias, T.K. Sen, Removal of zinc metal ion (Zn2+) from its aqueous solution by kaolin clay mineral: a kinetic and equilibrium study, Colloids Surf. A: Phys. Eng. Aspects, 348 (2009) 100–108.

Supplementary material

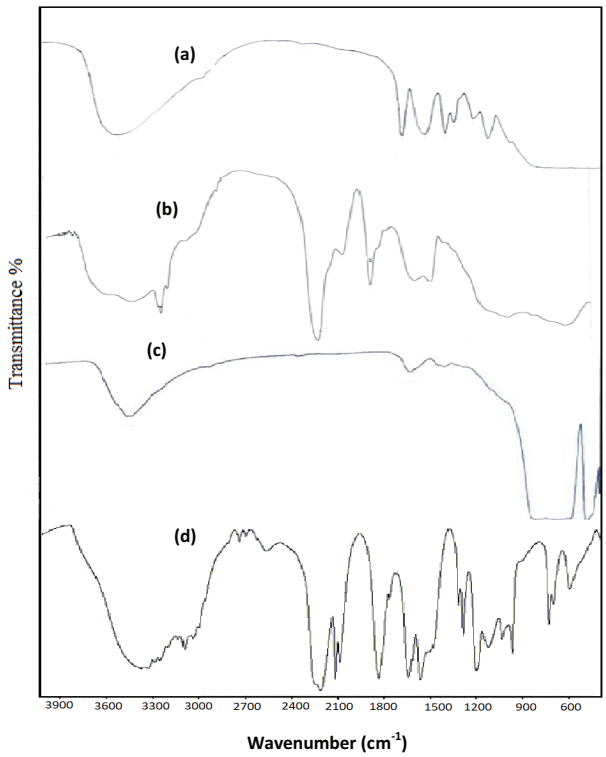

Fig. 1S. The FTIR spectrum for (a) AlO-AM, (b) AlO-AP, (c) Al_2O_3 and (d) acrylic acid.

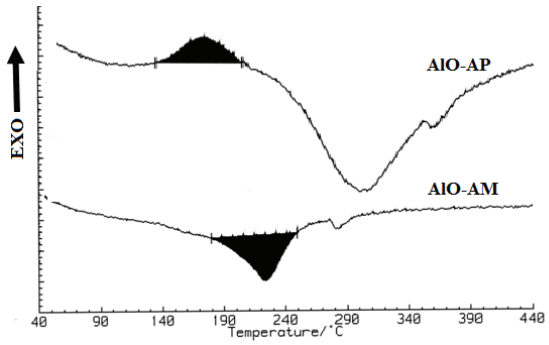

Fig. 2S. The DSC thermogram of trace for AlO-AM and AlO-AP.

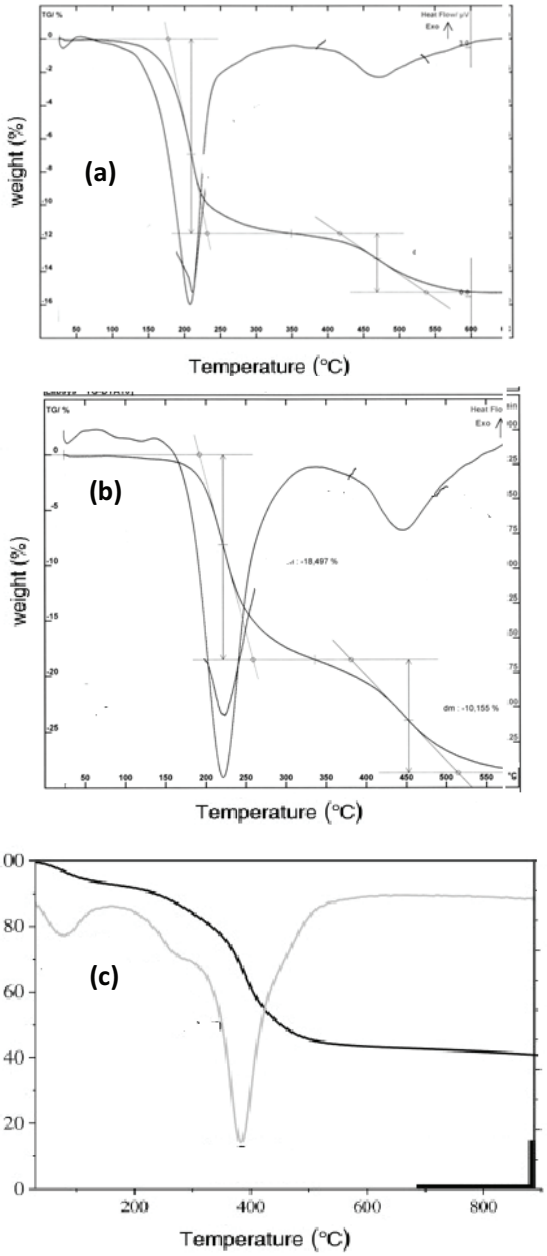

Fig. 3S. TG and DTG thermograms of trace for (a) AlO-AM, (b) AlO-AP and (c) polyacrylic acid.

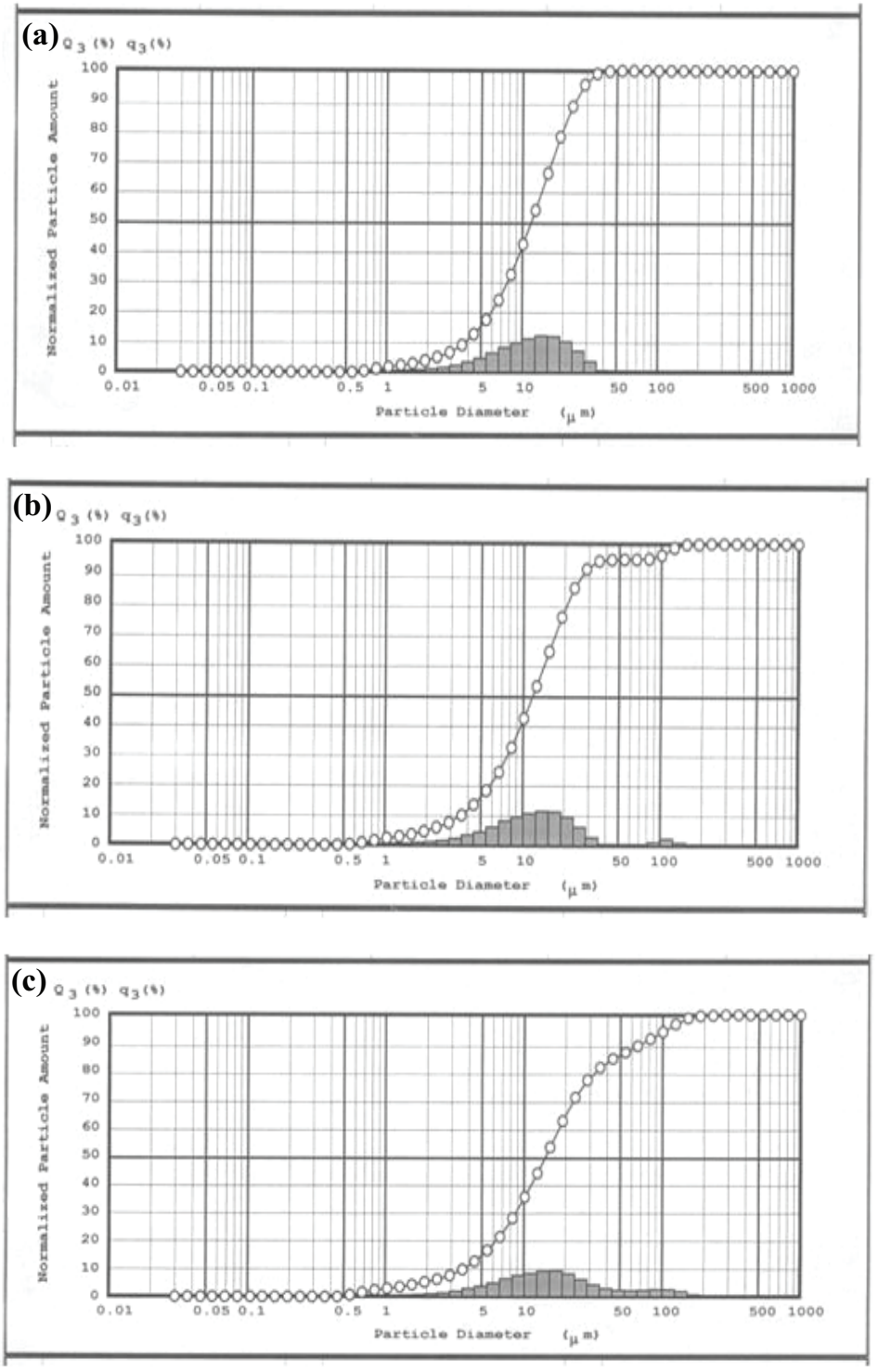

Fig. 4S. Particle size distribution of (a) AlO, (b) AlO-AM and (c) AlO-AP.